Available online at www.sciencedirect.com
SCIENCE DIRECT®

Journal of the European Ceramic Society 24 (2004) 1473–1477

www.elsevier.com/locate/jeurceramsoc

Characterization of $Ba(Ti,Zr)O_3$ ceramics sintered under reducing conditions

Christiane Hofer[a,*], René Meyer[a], Ulrich Böttger[a], Rainer Waser[a,b]

[a]*Institut für Werkstoffe der Elektrotechnik II, RWTH Aachen, D-52056 Aachen, Germany*
[b]*IFF/EKM, Forschungszentrum Jülich, D-52425 Jülich, Germany*

Abstract

Over the past few years, lead-free relaxor dielectrics have become particularly interesting for industrial applications. Due to the use of low cost base metal electrodes (BME), reductive sample sintering is required. This contribution refers to the influence of reducing sintering atmospheres on the dielectric behaviour of Mn-doped $Ba(Ti_xZr_{1-x})O_3$ ceramics with different Zr-contents (x = 0–100 at.%). It was studied by impedance spectroscopy in the temperature range $T = -150$–300 °C and the frequency range $f = 5$ mHz–10 MHz. For the interpretation of the impedance spectra we used an equivalent electrical circuit to separate bulk from grain boundary or electrode contributions, respectively. It was found that reductive sintering decreases the maximum dielectric constant by approx. 20%. Further, a T_{Curie} shift towards lower temperatures was observed. In contrast to materials sintered under oxidizing conditions, reduced sintered samples showed a plateau in the T_{Curie} versus Zr-content plot, derived from the Curie–Weiss behavior of the bulk in the cubic phase.

Keywords: $BaTiO_3$ and titanates; Electrical properties; Impedance; Perovskites; Relaxor

1. Introduction

High κ relaxor materials like $Ba(Ti,Zr)O_3$ with broad phase transitions are often used for dielectrics in commercial capacitor applications. Another requirement for the dielectrics is to be lead free, because of environmental aspects. BTZ fulfils the demand of lead freeness. But, with 120 °C the Curie temperature of $BaTiO_3$ is far over the average working temperature of most multilayer capacitors (MLC)-applications. The maximum of the permittivity ε_r of an idealized ferroelectric specimen could be described by the Curie–Weiss-law [Eq. (1)]:

$$\varepsilon_r = C_W/(T - T_{Curie}) \tag{1}$$

C_W denotes the curie constant, and T_{Curie} is the point were the extrapolation of $1000/\varepsilon_r$ intersects the abscissa (Fig. 1).

Addition of Zr shifts the T_{Curie} from 120 °C for as sintered BTO samples to −100 °C for BTZ-40 samples and results in a more diffuse phase transition of second order.[1] In order to reduce production costs of MLCs, base metal electrodes (BME, e.g. Ni) are appointed. The use of BME requires a reducing sintering atmosphere to prevent an oxidation of the electrodes. Reductive processing conditions are accompanied with an increase of losses in the dielectrics. The losses increase due to the forming of large numbers of electrons in pure BTZ in accordance with the following chemical equilibrium formula[2]:

$$O_O^x \rightleftharpoons 2e' + V_{\ddot{O}} + 0.5 \cdot O_2(g) \tag{2}$$

respectively the below stated mass action Eq. (3)

$$K = n^2 \cdot \left[V_{\ddot{O}}\right] \cdot p(O_2)^{0.5} \tag{3}$$

In formula (2) and (3) O_O^x denotes an oxygen ion on the regular lattice site, e' stands for an electron, $\left[V_{\ddot{O}}\right]$ for the oxygen vacancy concentration, K is the mass

* Corresponding author. Tel.: +49-241-807-817; fax: +49-241-8888-300.
E-mail address: hofer@iwe.rwth-aachen.de (C. Hofer).

0955-2219/$ - see front matter © 2003 Elsevier Ltd. All rights reserved.
doi:10.1016/S0955-2219(03)00573-9

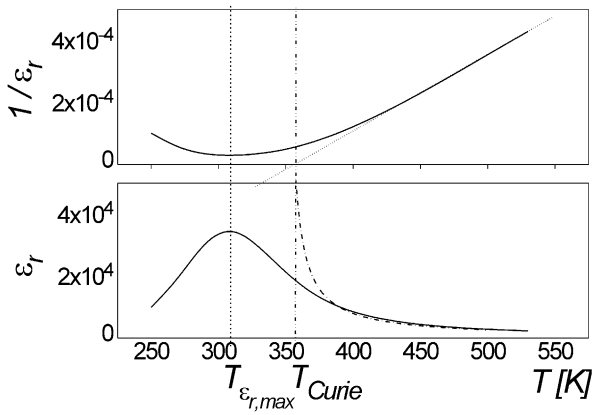

Fig. 1. Extrapolation of $1/\varepsilon_r$ and ε_r for MnBT to define T_{Curie} and $T(\varepsilon_{r,\max})$.

action constant, n stands for the electron concentration and $p(O_2)$ denotes the oxygen partial pressure. In Eq. (3) $\left[V_O^{\cdot\cdot}\right]$ is fixed by the net concentration of impurity and intrinsic acceptor $\left[A^{'}\right]_{\mathrm{imp}}$ states $\left[V_O^{\cdot\cdot}\right] \approx \left[A^{'}\right]_{\mathrm{imp}}$. Therefore Eq. (3) can be transformed to Eq. (4), where the dependence of the electron concentration of the $p(O_2)$ clearly can be seen.

$$K = n^2 \cdot [A]_{\mathrm{imp}} \cdot p(O_2)^{0.5} \Rightarrow\ n = \sqrt{\frac{K}{[A]_{\mathrm{imp}}}} \cdot p(O_2)^{-1/4} \qquad (4)$$

Caused by oxygen losses during the firing process the formation of conducting electrons give rise to very poor insulation resistances.[3] By additional incorporation of extrinsic acceptor ions in the perovskite lattice $[A]_{\mathrm{extr}} \gg [A]_{\mathrm{imp}}$ the conducting electrons can be trapped effectively and the insulating character of the dielectric could be restored.[2] Hence, doping the ceramics with acceptors results in an increase of resistance, whereby the acceptors were charge compensated by oxygen vacancies Eq. (5).[4–6]

$$\left[V_O^{\cdot\cdot}\right] \approx \left[A^{'}\right]_{\mathrm{extr}} \approx [Mn], \qquad (5)$$

where $[Mn]$ denotes the concentration of Mn-ions that were used as acceptor dopant in this study.

This letter reports on the influence of the sintering atmosphere on the dielectric and ferroelectric properties. We compared the reductive sintered samples and reoxidized samples with the values for oxidized sintered samples from literature.

2. Experimental procedure

2.1. Preparation

The acceptor-doped BTZ-bulk ceramics were prepared with 2 at.% B-site excess by the standard mixed oxide route, pursuant to Eq. (6):

$$\mathrm{MnCO_3} + \mathrm{BaCO_3} + (1\text{-}x)\mathrm{TiO_2} + x\mathrm{ZrO_2} \rightarrow \mathrm{Ba(Ti_{0.99-}}_x\mathrm{Mn_{0.01}Zr}_x\mathrm{)_{1.002}O_3} + \mathrm{CO_2} \qquad (6)$$

To receive an average grain size of $d < 0.5$ μm the $MnCO_3$ powder was milled in isopropanol using Y-stabilized ZrO_2 balls on a roller bank for 24 h. After this milling step TiO_2, ZrO_2, $BaCO_3$ where added and mixed for 25 h (1 h ball mill and 24 h roller bank). Subsequently, the powder was calcined for 6 h at 1300 °C in air and milled again for 1 h on the ball mill and 3 h on the roller bank. Afterwards 0.4 at.% SiO_2 was added as sintering aid and the powders were pressed to green bars. The subsequent firing step was performed at 1360 °C for 6 h in a moist reductive atmosphere (2% H_2/98% Ar). The received density of the samples is between 96 and 98% of the theoretical values.

After sintering the bars were cut in slices of 500 μm in thickness, lapped and polished. A part of the samples was post-annealed in air for 8 h at 1000 °C to study the influence of the oxygen partial pressure on the dielectric behavior. The respective $p(O_2)$ is shown in Table 1:

For the electrical characterization, electrodes consisting of 200 nm thick Ag and 50 nm thick Au films were evaporated. A 10 nm NiCr film was used to overcome the adhesion problems of the electrode.

3. Characterization

The samples were characterized in view of phase formation, microstructure, and dielectric properties. XRD analysis confirm the formation of $BaTiZrO_3$. Other second phases were not found within the resolution of the setup. Grain size was determined by optical microscopy and SEM of samples etched with a HCl-HF mixture or thermally, respectively. Fig. 2a) shows a micrograph of a thermally etched MnBTZ-30 sample with average grain sizes between 2–6 μm and a homogenous microstructure.

The dielectric measurements were performed by using impedance analysis techniques (NOVOCONTROL Broadband Dielectric Spectrometer). Measurements of the absolute value of the impedance $|\underline{Z}|$ and the phase φ were executed on Mn-doped BTZ-samples with different Zr-contents and thermal treatments. For these measurements, the frequencies ranged from 5 mHz to

Table 1
Frozen-in states of the untreated and annealed samples

Treatment	As sintered in H_2/Ar	Post-annealed in air
$p(O_2)$ [bar]	5×10^{-17}	0.2

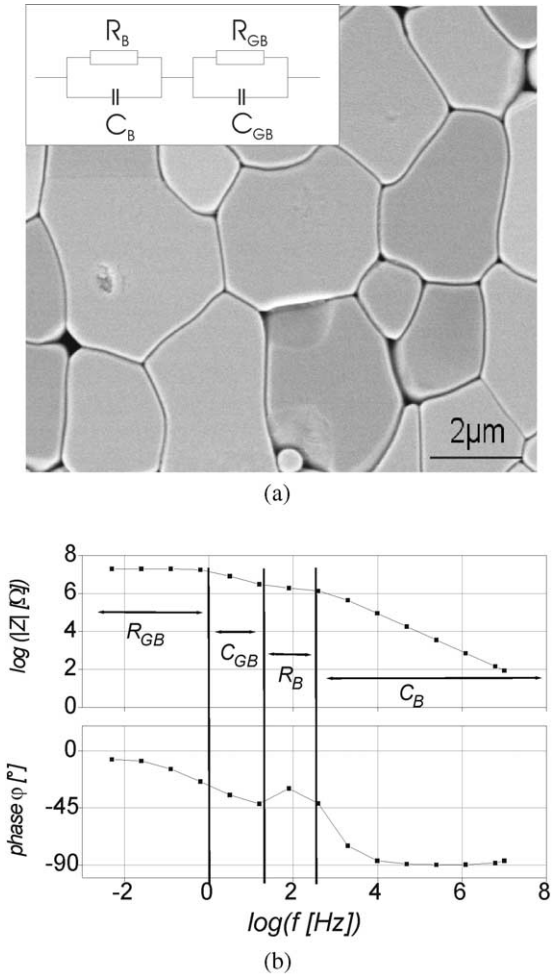

Fig. 2. (a) Microstructure of a thermally etched MnBTZ-30 sample. Inset: Equivalent electrical circuit consisting of two serial *RC* elements representing bulk and grain boundary contribution. (b) Measurement of $|\underline{Z}|$ with marked regions for R_{GB}, C_{GB}, R_B, and C_B.

10 MHz at temperatures between 123 and 573 K (20 K steps).

4. Results and discussion

As shown in the double-logarithmic plot of $|\underline{Z}|$, and in the plot of the phase φ in Fig. 2), sections with different slopes were found. The sections with a slope near one are interpreted as a capacitive behaviour, and the sections with a slope near zero as an ohmic behaviour. The complex dielectric response of the samples was represented by a serial association of 2 *RC*-cells. Clearly visible transitions are only found for reduced sintered specimen. The post-annealed samples (not presented) do not show such a pronounced behaviour.

One *RC*-cell represents the bulk contribution of the sample. The other *RC*-cell might be associated with grain boundary or electrode properties, respectively. The separation of the impedance $\underline{Z}$ into bulk and grain boundary/electrode parts leads to the following Eq. (7).

$$\left|\underline{Z}\right| = \sqrt{\left(\frac{R_B}{1+(\omega\cdot R_B\cdot C_B)^2}+\frac{R_{GB}}{1+(\omega\cdot R_{GB}\cdot C_{GB})^2}\right)^2 + \left(\frac{R_B^2\cdot\omega\cdot C_B}{1+(\omega\cdot R_B\cdot C_B)^2}+\frac{R_{GB}^2\cdot\omega\cdot C_{GB}}{1+(\omega\cdot R_{GB}\cdot C_{GB})^2}\right)^2} \tag{7}$$

Eq. (8) describes the phase.

$$\varphi = \tfrac{180}{\pi}\arctan\left(\frac{\mathrm{Im}\left\{\underline{Z}\right\}}{\mathrm{Re}\left\{\underline{Z}\right\}}\right) \tag{8}$$

The values of R_B (ohmic part of the bulk), C_B (capacitive part of the bulk), R_{GB} (ohmic part of the grain boundary) and C_{GB} (capacitive part of the bulk) are obtained by fitting the Eq. (7) to the experimental impedance data. In the following we will discuss the impact of the sintering atmosphere as well as the temperature and Zr-content on the dielectric and ferroelectric properties.

T_{Curie} was acquired from the $C_B(T)$ branch in the cubic phase. Fig. 3 shows T_{Curie} versus Zr-content for the acceptor-doped reduced sintered specimen in comparison with acceptor-doped reoxidized and undoped in air sintered samples. A partial substitution of Ti by Zr leads, for reduced sintered samples, to a decrease of the Curie point with increasing Zr-content (Fig. 3), which is in accordance to literature data samples processed in air.[7,8] T_{Curie} for the reduced sintered samples is much lower than for oxidized sintered samples. Further, a plateau occurs for Zr-contents between 10 and 20 at.%. For reoxidized specimen we observed a shift of T_{Curie} towards in air sintered samples and the plateau vanishes. The values for the Mn-doped post-annealed specimen resemble those for undoped oxidized sintered values taken from literature. Already here a large influence of the oxygen partial pressure can be seen.

In the ferroelectric phase below T_{Curie} a decrease of $\varepsilon_{r,\max}$ with increasing Zr-content (Fig. 4) is observed. After the post-annealing step the $\varepsilon_{r,\max}$ considerably is increased. We also found that ε_r decreases faster as a function of Zr-content for the as sintered samples than for the air-annealed ones. Obviously, exposing the sample to different oxygen partial pressures at high temperatures influence the polarizability of the material both in the paraelectric and in the ferroelectric phase.

To understand the change of the dielectric properties we will consider the point defect chemistry already

mentioned at the beginning. A first estimation made in Eq. (5) was that the concentration of the oxygen vacancies is kept constant by the acceptor concentration of Mn. In a refined approach a valence change of Mn accompanied with a changing concentration of oxygen vacancies will be considered (Fig. 5). Since Mn is heterovalent, it changes its valence state with the oxygen partial pressure. Hence, the set of the defect equations has to be extended by Eqs. (9) and (10).

$$e' + Mn_{Ti}^{x} \rightleftharpoons Mn_{Ti}' \tag{9}$$

$$e' + Mn_{Ti}' \rightleftharpoons Mn_{Ti}'' \tag{10}$$

The lowest valence state of the acceptor ions occurs at very reducing conditions. Then, the Mn is charged 2+. At low temperatures, Mn_{Ti}''-$V_O^{\cdot\cdot}$ defect-associated dipoles may also form. With increasing $p(O_2)$ the valence state of Mn increases. The concentration of oxygen vacancies decreases and at the same time the coulomb attraction between Mn_{Ti}'-$V_O^{\cdot\cdot}$ becomes weaker. For highest oxygen activities Mn^{4+} becomes the majority valence state. In comparison to reduced sintered samples the concentration of oxygen vacancies decreased by one order of magnitude. This value is similar to the oxygen vacancy concentration of impurity acceptor doped nominal undoped samples.

We assume that the $p(O_2)$-dependent variation of the oxygen vacancy concentration may evoke the observed $p(O_2)$ dependent changes in the dielectric and ferroelectric properties. At lower temperatures, oxygen vacancies may affect domain wall motion by screening of the polarization charge. A formation of mechanical barriers against the domain walls by oxygen vacancies, so called domain wall pinning, might also stabilize the domain configuration (Fig. 6). For higher temperatures where the domain walls do not exist anymore, the

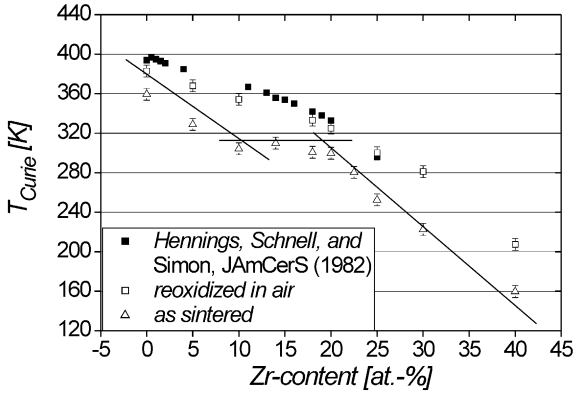

Fig. 3. Comparison between T_{Curie} of undoped BTZ (values from literature[1]) and Mn-doped BTZ (measured as sintered and air-annealed). As sintered samples reveal a characteristic plateau of T_{Curie} between 10 at.% and 20 at.% Zr.

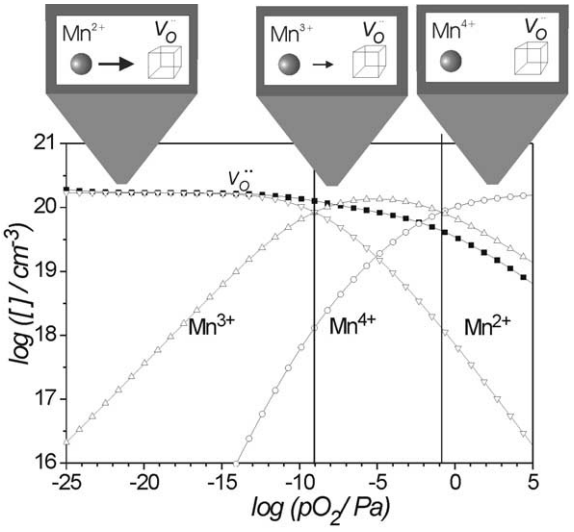

Fig. 5. Simulation of Mn-valence state as a function of $p(O_2)$.

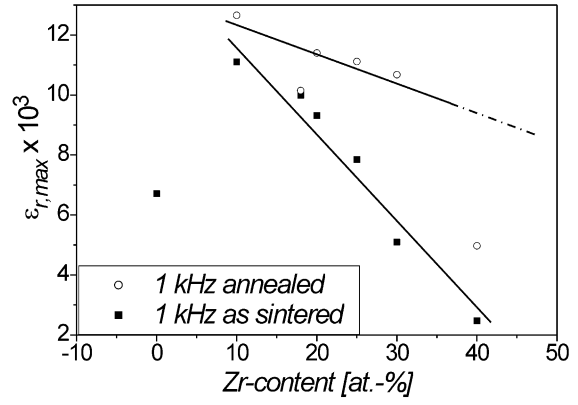

Fig. 4. $\epsilon_{r,max}$ versus Zr-content for reduced sintered samples and air-annealed samples.

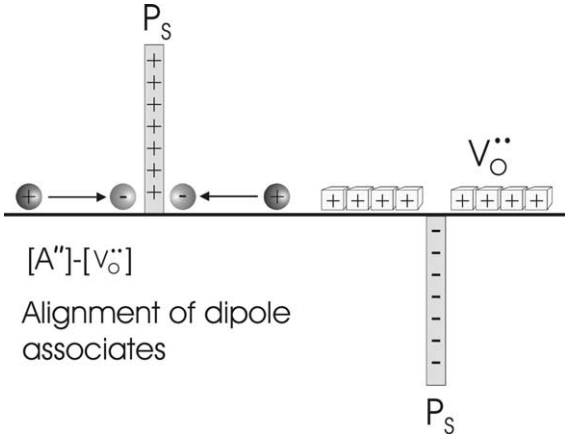

Fig. 6. Sketch of domain wall screening by oxygen vacancies or defect dipoles.

polarizability of the dielectric matrix might also be lowered by the presence of oxygen vacancies.

Surprisingly, the behaviour of T_{Curie} for Mn-doped post-annealed and undoped oxidized sintered samples is rather similar. We attribute this observation to the predominant 4+ valance state of Mn for oxidizing conditions. Since Mn^{4+} substitutes Ti^{4+} it will act rather similar to regular the lattice ion.

5. Conclusions

Mn acceptor doped BTZ ceramics with different Zr contents were investigated with regards to $p(O_2)$. The samples were sintered in reductive atmosphere, a part of them reoxidized in air and characterized electrically by means of impedance spectroscopy.

We found a large influence of the $p(O_2)$ on the permittivity and the curie temperature and therefore on the ferroelectric and dielectric properties of the material. For increasing $p(O_2)$, the $\varepsilon_{r,max}$ decreases, and Curie temperature T_{Curie} is shifted to higher temperatures. We attribute the change in the dielectric behaviour with $p(O_2)$ to a change of the valence state of Mn and hence, a change in the concentration of oxygen vacancies. Increasing $p(O_2)$ causes an increase of higher valent Mn ions and a decrease of the oxygen vacancies.

References

1. Hennings, D., Schnell, A. and Simon, G., Diffuse ferroelectric phase transitions in Ba(Ti $_{1-y}$, Zr $_{y}$)O_3 ceramics. *J. Am. Ceram. Soc.*, 1982, **65**, 539–544.
2. Weber, U., Hagenbeck, R., Waser, R., Schreinemacher, H., Hansen, P. and Hennings, D. Influence of acceptor-donor co-doping on electrical properties of Ba(Ti, Zr)O_3 based ceramic multilayer capacitor materials.
3. Schaumburg, H. and Keramik, B. G., Teubner Verlag, Stuttgart, 1994
4. Waser, R. and Baiatu, T. and Härdtl, K. H., dc Electrical degradation of perovskite-type titanates: I, ceramics. *J. Am. Ceram. Soc.*, 1990, **73**(6), 1645–1653.
5. Waser, R., Baiatu, T. and Härdtl, K. H., dc Electrical degradation of perovskite-type titanates: II, single crystals. *J. Am. Ceram. Soc.*, 1990, **73**(6), 1654–1662.
6. Waser, R., Baiatu, T. and Härdtl, K. H., dc Electrical degradation of perovskite-type titanates: III, a model of the mechanism. *J. Am. Ceram. Soc.*, 1990, **73**(6), 1663–1673.
7. Hansen, P., Hennings, D. and Schreinemacher, H., Dielectric properties of acceptor-doped (Ba,Ca)(Ti,Zr)O_3 ceramics. *J. Electroceramics*, 1998, **2**, 85–94.
8. Mitsui, T., *Landoldt-Börnstein: Zahlenwerte und Funktionen aus Naturwissenschaften und Technik, Band 3: Ferro- und Antiferroelektrische Substanzen*. Springer Verlag, Berlin, Heidelberg, New York, 1969.